Scientific Research Publishing

Journal of Modern Physics, 2024, 15, 2193-2219
https://www.scirp.org/journal/jmp
ISSN Online: 2153-120X
ISSN Print: 2153-1196

Derivation of Cylindrical Internal-Surface Acoustic Waves and Their Small Gravity Effect

Philipp G. Kornreich[1,2]

[1]1090 Wien, Austria,
[2]King of Prussia, PA, USA
Email: pkornrei@syr.edu

How to cite this paper: Kornreich, P.G. (2024) Derivation of Cylindrical Internal-Surface Acoustic Waves and Their Small Gravity Effect. *Journal of Modern Physics*, **15**, 2193-2219.
https://doi.org/10.4236/jmp.2024.1512088

Received: September 19, 2024
Accepted: November 9, 2024
Published: November 12, 2024

Copyright © 2024 by author(s) and Scientific Research Publishing Inc.
This work is licensed under the Creative Commons Attribution International License (CC BY 4.0).
http://creativecommons.org/licenses/by/4.0/

Open Access

Abstract

The properties of Cylindrical Internal-Surface Acoustic Waves (CISAW) propagating on the inside surface of a high purity fused quartz tubular fiber are derived from basic principles using a variational method. The CISAW consist of Energy Momentum Packets (EMP) moving in a looping motion. The EMP have mass and are affected by gravity similar to a pendulum bob. The effect of gravity on CISAW is much larger than the effect of gravity in a light wave. Therefore, one can build much smaller CISAW Interferometer Gravity wave Observatories (CIGO) than the present km size Light Interferometer Gravity wave Observatories (LIGO). An array of CIGO can be used to detect gravity wave images. Since the wavelength of gravity waves is much larger than the expected spacing between CIGO array elements this would result in sub-wavelength images. It would be interesting to determine what new discoveries could be made using such an array.

Keywords

Elastic Constant Tensor, Continuum Mechanics, Lagrangian, Wave Equation, Surface Acoustic Waves, Newtonian Gravity

1. Introduction and Summary

The *properties of Cylindrical Internal-Surface Acoustic Waves (CISAW) propagating on the inside surface of a high purity fused quartz tubular fiber and its gravity effect are derived in this study from basic principles. The CISAW have a small group velocity and the effect of gravity on CISAW propagation is large. Therefore, one can build an array of CISAW based gravity wave detectors that are able to observe gravity wave images.*

I was unable to find descriptions in scientific literature of the modes of CISAW

or its gravity effect. The wavelength of the CISAW is of the same order of magnitude as the fiber inside circumference. The CISAW are similar to Rayleigh waves [1] [2]. The effect of gravity on CISAW is analyzed in this study. These fibers are designed for Cylinder Internal-Surface Acoustic Wave propagation, and not for light wave propagation.

This analysis uses the Earth's surface as an approximate Inertial Reference Frame. A point on the surface of the Earth moves with an approximately constant linear velocity during the time it takes an Acoustic Surface Wave to propagate through the tubular fiber.

Here a Classical Continuum Mechanics model is used. An infinitesimal mass in a solid consists of an infinitesimal volume with a sufficient number of atoms to be considered as a continuum. This infinitesimal mass does not move more than an infinitesimal distance. But each infinitesimal mass bumps against the next infinitesimal mass etc. This slightly compresses the infinitesimal mass. In each collision it transfers Kinetic Energy and Momentum and when it re-expands, it also transfers Elastic Potential Energy to the next infinitesimal mass. These Energy Momentum Packets (EMP) can travel any distance. The EMP's have mass. Therefore, in this study the displacement vector u describes the position of the EMP's, not the position of the mass increments. The displacement is a wave. The Quantum Mechanical version of the CISAW are a type of Phonons. The displacement of the EMP's have longitudinal and transverse components.

If one neglects the small effect of the air, there is no force on the inside surface of the fiber tube on which the CISAW propagates. Therefore, the stress in the solid produced by the longitudinal and transverse displacement components has to be zero on the inside surface of the tubular fiber. This couples the longitudinal and transverse displacement components to form Elastic Surface Wave modes.

The longitudinal displacement component wave is shifted by 90 degrees with respect to the transverse component wave. When the transverse displacement component wave is zero and the longitudinal displacement component wave is at its maximum, the total displacement is longitudinal. When the longitudinal displacement component wave is zero and the transverse displacement component wave is at its maximum, the total displacement is transverse to the inside surface. But at the next zero value of the transverse displacement component wave the longitudinal component wave is at its maximum negative value, therefore, the total displacement is moving in the reverse direction. This makes the total displacement to move in a loop along the wave. Thus, the EMP's in SAW's, move in loops along the wave.

Over the distance of a few meters on Earth the gravitational force is constant in the "down" direction. But only a component of the gravity force acts on an object in the direction of its motion. If the object periodically changes direction, the component of the gravity force in the direction of the object motion will also change periodically. This is how the gravity force acts on a pendulum bob. The component of the gravity force acts in the direction of the pendulum bob motion. This gravity force component has a non-zero value during the downwards swing of the

pendulum bob, and it is equal to zero when the pendulum bob moves horizontally at the bottom of its swing.

As described above the EMP's have mass and are affected by gravity. When an EMP moves longitudinally on top and bottom of the loop, it does not interact with gravity. When an EMP moves vertically in the loop, its interaction with gravity is a maximum. Therefore, the part of the gravitational force acting on the EMP's have a similar looping wave motion as the EMP's. Thus, SAW's interact with gravity. The interaction of the energy momentum packets in the SAW's is similar to the interaction of the pendulum bob with gravity. The effect of gravity on the EMP's of CISAW's is also similar to the effect of gravity on Ocean Surface Waves (OSW) [3] on a deep ocean.

There are interactions with the curvature of space-time. The small effect of the curvature of space time on CISAW's is neglected here.

I think this is the first published analysis of the modes of CISAW's. I was unable to find any analysis in literature of Surface Acoustic Waves propagating on the inside surface of a cylinder. But, described below, is research somewhat related to this study:

I remember Dr. Stephen Tehan and Stephen Wanuga at the Electronics Laboratory of the General Electric Company in Syracuse, NY about 1975 propagated Surface Acoustic Waves on the inside surface of simple tubular fused quartz fibers. They wanted to use CISAW pulses propagating in the tubular fibers as a digital memory. But I was unable to find any calculations or other documentation of this work. The CISAW's propagated with relatively little amplitude loss.

Wen Wang *et al.* [4] of the Acoustic Institute of the Chinese Academy of Science developed a Surface Acoustic Wave (SAW) based gyroscope on a LiTaO5 wafer. The gyroscope consists of two SAW transducers and two resonators in a loop on a piezoelectric $LiTaO_5$ wafer. It uses the carioles force. The infinitesimal energy momentum packets under the transducers have inertia and tend to move in a straight line while the gyroscope moves with the Earth's rotation. This carioles force effect on the SAW is similar to the effect of gravity acting on the SAW in the tubular fiber described in this study. There are many papers published describing SAW Devices on piezoelectric wafers such as [5].

R. E. Bunney *et al.* [6] propagated Surface Acoustic Waves on the outside of stainless steel and various aluminum alloy cylinders submerged in water. These cylinders had diameters of 10 to 400 times of the acoustic wavelengths.

Denos C. Gazis [7] [8] describes Elastic Waves in the material of hollow cylinders. He calculates the modes of Longitudinal waves, Equivoluminal Lame Type elastic waves, and Torsional elastic waves. All these elastic modes are bulk waves propagating in a solid material. In longitudinal and shear elastic waves where the displacements are horizontal or vertical and therefore, the EMP's don't interact with gravity in the Newtonian model. None of these bulk waves exhibit looping motion of the EMP's. Only Surface Acoustic Waves, Rayleigh waves, exhibit looping motion of the EMP's that couple to gravity. The EMP's circular motion in

Torsional waves might interact with gravity. However, since the Torsional waves are also on an outside surface, they are not suitable for many applications.

The gravity wave detectors based on CISAW interferometers can have a large effect on astronomical observations. The effect of gravity on CISAW's is much larger than on light waves used in the current (year 2024) gravity wave detectors of the Light Interferometer Gravity-wave Observatory (LIGO) experiment [9]-[16]. Therefore, interferometer gravity wave detectors based on CISAW's would be much smaller than gravity wave detector interferometers based on light waves. This would facilitate the building of CISAW gravity wave detector arrays. These Gravity wave interferometer arrays would for the first time be able to observe space-time curvature mode images. Gravity waves detected to date, have frequencies of a few hundred cycles or wavelengths of about 43 km to 1500 km [9]-[16]. The detectors in these arrays would be spaced at intervals that are much less than the wavelengths of a gravity wave. These arrays would perform sub-wavelength imaging [17] with gravity waves. Sub-wavelength imaging is currently used in photolithography in nanometer-scale semiconductor device manufacturing. It is interesting what future discoveries can be made using gravity-wave imaging.

2. Derivation of Cylindrical Internal-Surface Acoustic Waves

This analysis uses the Earth's surface as an approximate Inertial Reference Frame. The propagation time of the elastic wave in the 1257 meter long fiber was approximately 0.430321 seconds. A point on the surface of the Earth moved approximately 141.132 m during this time at a latitude of 45 degrees. This represents only 31.295 micro-radians of arc or 1.79305 milli-degrees of the Earth's rotation. Therefore, during this period it can be assumed that a point on the surface of the Earth moves with an approximate constant linear velocity. The Earth also moves approximately linearly in its orbit during this time period.

The analysis starts with the symmetrized second rank strain tensor components $\Sigma_{\alpha\beta}$ which have the following form:

$$\Sigma_{\alpha\beta} = \frac{1}{2}\left(\partial_\beta u_\alpha + \partial_\alpha u_\beta\right) \tag{1}$$

where $u_\alpha \ni \mathbb{R}(3)$ is a displacement component of an infinitesimal Energy Momentum Packet

(EMP), $x_\alpha \ni \mathbb{R}(3)$ is a coordinate component, where $\alpha = 1,2,3$ and $\partial_\alpha = \dfrac{\partial}{\partial x_\alpha}$. As described in the introduction it is the EMP's that travel in the CISAW.

Next, to obtain the elastic properties of the fused silicon material, the components of the second rank stress tensor elements $\sigma_{\alpha\beta}$ are expanded to first order in the strain tensor elements $\Sigma_{\gamma\delta}$:

$$\begin{aligned} &\text{a)}\ \sigma_{\alpha\beta} = \frac{\partial\sigma_{\alpha\beta}}{\partial\Sigma_{\gamma\delta}}\Sigma_{\gamma\delta} + \cdots \\ &\text{b)}\ \sigma_{\alpha\beta} = c_{\alpha\beta\delta\gamma}\Sigma_{\gamma\delta} + \cdots \end{aligned} \tag{2}$$

where the summation over the repeated indices is implied. Here, we retain only the linear expansion terms where $c_{\alpha\beta\gamma\delta}$ is a component of the covariant fourth rank elastic constant tensor of the fused silicon material. There exists much smaller higher order non-linear elastic constant terms that contribute to the losses mentioned in the introduction. The effect of gravity is represented by the gravitational potential density ϕ. In the Newtonian model used here, the gravitational potential density is represented by the fused quartz material density ρ times the acceleration of gravity g times the elevation $h(\boldsymbol{u})$ of the EMP.

$$\phi \Rightarrow \rho g h(\boldsymbol{u}) \tag{3}$$

The properties of the CISAW are described by a wave equation. In order to derive this wave equation, a Newtonian Mechanics Lagrangian density $\mathcal{L}$ is hypothesized. This is the first hypothesis. The Lagrangian density $\mathcal{L}$ is the difference between the Kinetic Energy density, the Elastic and the gravitational Potential Energy densities.

$$\mathcal{L} = \frac{1}{2}\rho \dot{u}_\alpha \dot{u}_\alpha - \frac{1}{2}\Sigma_{\alpha\beta} c_{\alpha\beta\gamma\delta} \Sigma_{\gamma\delta} - \rho g h(u_\alpha) \tag{4}$$

The gravitational potential energy density could have the form $\phi \approx -\dfrac{\rho MG}{r}$ where ρ is the mass density, M is a mass, G is Newton's gravitational constant, and r is the distance between the centers of mass of objects.

Substituting Equation (1) into Equation (4) in order to formulize the Lagrangian density in terms of the displacement components:

$$\begin{aligned}\mathcal{L} = {} & \frac{1}{2}\rho \dot{u}_\alpha \dot{u}_\alpha - \frac{1}{2}\partial_\beta u_\alpha c_{\alpha\beta\gamma\delta} \partial_\delta u_\gamma - \frac{1}{2}\partial_\alpha u_\beta c_{\alpha\beta\gamma\delta} \partial_\delta u_\gamma \\ & - \frac{1}{2}\partial_\beta u_\alpha c_{\alpha\beta\gamma\delta} \partial_\gamma u_\delta - \frac{1}{2}\partial_\alpha u_\beta c_{\alpha\beta\gamma\delta} \partial_\gamma u_\delta - \rho g h(u_\alpha)\end{aligned} \tag{5}$$

At this point the Euler Lagrange [18] equation could have been used to obtain a wave equation. But, I prefer the derivation from basic principles using a variational process. This requires the forming of a constant action integral I which states that the integral of the Lagrangian density over the time period and volume considered is a constant. In this study there is nothing outside the volume and time period considered. Therefore, an integral over this volume and time period is a constant, and the variation of this integral is equal to zero.

We form an action integral $\mathcal{I}$ over both the time period and volume considered.

$$\begin{aligned}\mathcal{I} = {} & \frac{1}{2}\int_{\tau_a}^{\tau_b} \rho \dot{u}_\alpha(x_\mu, \xi, \tau) \dot{u}_\alpha(x_\mu, \xi, \tau) \mathrm{d}\tau \\ & - \frac{1}{2}\int_{s_a}^{s_b} \Big\{ c_{\alpha\beta\gamma\delta} \Big[\partial_\beta u_\alpha(x_\mu, \xi, \tau) \partial_\delta u_\gamma(x_\mu, \xi, \tau) \\ & + \partial_\alpha u_\beta(x_\mu, \xi, \tau) \partial_\delta u_\gamma(x_\mu, \xi, \tau) + \partial_\beta u_\alpha(x_\mu, \xi, \tau) \partial_\gamma u_\delta(x_\mu, \xi, \tau) \\ & + \partial_\alpha u_\beta(x_\mu, \xi, \tau) \partial_\gamma u_\delta(x_\mu, \xi, \tau) \Big] + 2\rho g h(u_\alpha) \Big\} \mathrm{d}v\end{aligned} \tag{6}$$

Because the analysis here uses three-dimensional space and time separately, the

action integral over time and the three spatial dimensions were performed separately. Here, dv is a volume increment in three-dimensions and s_a and s_b are the two surfaces at the start and end of the volume of integration respectively. Dummy variables $\tau \in \mathbb{R}(1)$ and $\xi \in \mathbb{R}(1)$ were introduced to facilitate the variation. The variation of the constant action integral is equal to zero.

$$\delta \mathcal{I} = 0 \tag{7}$$

The variation of the action integral was performed in **Appendix A**. We obtained a wave equation from Equation (A16) in **Appendix A**:

$$\begin{aligned} \rho \ddot{u}_\alpha = & \frac{1}{2}\Big[c_{\alpha\beta\gamma\delta}\partial_\beta\partial_\delta u_\gamma + c_{\gamma\beta\alpha\delta}\partial_\delta\partial_\beta u_\gamma + c_{\beta\alpha\gamma\delta}\partial_\delta\partial_\beta u_\gamma + c_{\gamma\beta\alpha\delta}\partial_\delta\partial_\gamma u_\beta \\ & + c_{\alpha\beta\gamma\delta}\partial_\beta\partial_\gamma u_\delta + c_{\delta\beta\gamma\alpha}\partial_\gamma\partial_\beta u_\delta + c_{\beta\alpha\gamma\delta}\partial_\beta\partial_\gamma u_\delta + c_{\delta\beta\gamma\alpha}\partial_\gamma\partial_\delta u_\beta \Big] \\ & + \rho g \frac{\partial h}{\partial u_\alpha} + \frac{1}{2}\frac{\partial^2 \phi}{\partial u_\alpha \partial u_\beta} u_\beta \end{aligned} \tag{8}$$

The change $\rho g \dfrac{\partial h}{\partial u_\alpha}$ of the gravity potential density $\rho g h$ with the displacement u_α of the EMP is the component of the gravity force in the direction of the EMP's motion. $\dfrac{\partial h}{\partial u_\alpha}$ is a dimensionless direction cosine that will be discussed later. There is a second-order smaller Newtonian gravity effect $\dfrac{1}{2}\dfrac{\partial^2 \phi}{\partial u_\alpha \partial u_\beta} u_\beta$ that was not part of this derivation. However, this second-order term is much smaller than the first order term, and is here neglected. This term is the effect of gravity on longitudinal and shear elastic waves.

In an isotropic material the Wave Equation is given in terms of the Lame constants [17]. In the next step we show that the wave equation, Equation (8) derived here is equal to this reported wave equation. The elastic constant tensors are symmetric in the first two indices $c_{\alpha\beta\gamma\delta} = c_{\beta\alpha\gamma\delta}$ and in the last two indices $c_{\alpha\beta\gamma\delta} = c_{\alpha\beta\delta\gamma}$.

$$\begin{aligned} \rho \ddot{u}_\alpha = & \frac{1}{2}\Big[4c_{\alpha\beta\gamma\delta}\partial_\beta\partial_\delta u_\gamma + c_{\gamma\beta\alpha\delta}\partial_\delta\partial_\beta u_\gamma + c_{\gamma\beta\alpha\delta}\partial_\delta\partial_\gamma u_\beta + c_{\delta\beta\gamma\alpha}\partial_\gamma\partial_\beta u_\delta \\ & + c_{\delta\beta\gamma\alpha}\partial_\gamma\partial_\delta u_\beta \Big] + \rho g \frac{\partial h}{\partial u_\alpha} \end{aligned} \tag{9}$$

Isotropic symmetry requires that we contract Equation (9) with respect to the indices, γ and δ to obtain:

$$\begin{aligned} \text{a)}\ \rho \ddot{u}_\alpha = & \frac{1}{2}\left(4c_{\alpha\beta\delta\delta} + c_{\delta\beta\alpha\delta} + c_{\delta\beta\delta\alpha}\right)\partial_\beta\partial_\gamma u_\gamma + \frac{1}{2}\left(c_{\delta\beta\alpha\delta} + c_{\delta\beta\delta\alpha}\right)\partial_\gamma\partial_\gamma u_\beta \\ & + \rho g \frac{\partial h}{\partial u_\alpha} \\ \text{b)}\ \rho \ddot{u}_\alpha = & \left(\lambda + \mu\right)\delta_{\alpha\beta}\partial_\beta\partial_\gamma u_\gamma + \mu\delta_{\alpha\beta}\partial_\gamma\partial_\gamma u_\beta + \rho g \frac{\partial h}{\partial u_\alpha} \end{aligned} \tag{10}$$

where the Lame constants in terms of the elastic constant tensor elements are:

$$\text{a)}\ \lambda\delta_{\alpha\beta} = 2c_{\alpha\beta\delta\delta} \qquad \text{b)}\ \mu\delta_{\alpha\beta} = \frac{1}{2}\left(c_{\delta\beta\alpha\delta} + c_{\delta\beta\delta\alpha}\right) \tag{11}$$

Equation (10b) can be written in vector form using the Lame constants λ and μ. The Lame constants for fused quartz are $\lambda = 15.87$ GPa and $\mu = 31.26$ GPa. The density of fused quartz is $\rho = 2200$ kg/m^3. The vector form of Equation (10b) is the wave equation for the EMP's[1] [19].

$$\rho\ddot{\boldsymbol{u}} = (\lambda+\mu)\nabla(\nabla\bullet\boldsymbol{u}) + \mu\nabla^2\boldsymbol{u} + \hat{\boldsymbol{a}}_\alpha\rho g\frac{\partial h}{\partial u_\alpha} \tag{12}$$

where bold fonts denote vectors. Here $\hat{\boldsymbol{a}}_\alpha$ is a unit vector in the direction of the EMP motion. Equation (12) can be rewritten using the vector calculus identity [19] $\nabla\times\nabla\times\boldsymbol{u} = \nabla(\nabla\bullet\boldsymbol{u}) - \nabla^2\boldsymbol{u}$ for $\nabla^2\boldsymbol{u}$.

$$\rho\ddot{\boldsymbol{u}} = (\lambda+2\mu)\nabla(\nabla\bullet\boldsymbol{u}) - \mu\nabla\times\nabla\times\boldsymbol{u} + \hat{\boldsymbol{a}}\rho g\frac{\partial h}{\partial u_\alpha} \tag{13}$$

At this point of the calculation, an attempt can be made to separate the displacement vector $\boldsymbol{u}$ into two parts:

$$\boldsymbol{u} = \boldsymbol{u}_\parallel + \boldsymbol{u}_\perp \tag{14}$$

where

$$\begin{aligned}&\text{a)}\ \text{Longitudinal component with } \nabla\times\boldsymbol{u}_\parallel = 0\\ &\text{b)}\ \text{Transverse component with } \nabla\bullet\boldsymbol{u}_\perp = 0\end{aligned} \tag{15}$$

Substituting Equation (14) into Equation (13), using Equation (15), and dividing the resulting equation by ρ.

$$\ddot{\boldsymbol{u}}_\parallel + \ddot{\boldsymbol{u}}_\perp = \frac{\lambda+2\mu}{\rho}\nabla(\nabla\bullet\boldsymbol{u}_\parallel) - \frac{\mu}{\rho}\nabla\times\nabla\times\boldsymbol{u}_\perp + \hat{\boldsymbol{a}}_\alpha g\frac{\partial h}{\partial u_\alpha} \tag{16}$$

The longitudinal and shear velocities squared are:

$$\begin{aligned}&\text{a)}\ \frac{\lambda+2\mu}{\rho} := v_\ell^2 \quad \text{Longitudinal velocity squared}\\ &\text{b)}\ \frac{\mu}{\rho} := v_s^2 \quad \text{Shear velocity squared}\end{aligned} \tag{17}$$

The longitudinal velocity $v_\ell = 5969.23933$ m per second and the shear velocity $v_s = 3769.494782$ m per second for fused quartz. Substituting Equation (17) into Equation (16).

$$\ddot{\boldsymbol{u}}_\parallel + \ddot{\boldsymbol{u}}_\perp = v_\ell^2\nabla(\nabla\bullet\boldsymbol{u}_\parallel) - v_s^2\nabla\times\nabla\times\boldsymbol{u}_\perp + \hat{\boldsymbol{a}}g\frac{\partial h}{\partial u_\alpha} \tag{18}$$

Making a transformation of variables to normal mode displacement vectors:

$$\text{a)}\ \boldsymbol{u} = \boldsymbol{u}_\parallel + \boldsymbol{u}_\perp \qquad \text{b)}\ \boldsymbol{s} = \frac{v_\ell^2}{v_\ell^2+v_s^2}\boldsymbol{u}_\parallel - \frac{v_s^2}{v_\ell^2+v_s^2}\boldsymbol{u}_\perp \tag{19}$$

Equation (19a) is a restatement of Equation (14). Here $\boldsymbol{u}$ is a wave displacement mode vector of an EMP and $\boldsymbol{s}$ is a stationary mode vector also of an EMP.

[1]At this point we change to vector notation which facilitates the use of cylindrical coordinates.

Inverting Equation (19)

$$\begin{aligned} &\text{a)}\ \boldsymbol{u}_{\parallel}(t,\boldsymbol{r}) = \boldsymbol{s}(\boldsymbol{r}) + \frac{v_s^2}{v_\ell^2 + v_s^2}\boldsymbol{u}(t,\boldsymbol{r}) \\ &\text{b)}\ \boldsymbol{u}_{\perp}(t,\boldsymbol{r}) = -\boldsymbol{s}(\boldsymbol{r}) + \frac{v_\ell^2}{v_\ell^2 + v_s^2}\boldsymbol{u}(t,\boldsymbol{r}) \end{aligned} \tag{20}$$

By substituting Equation (20) into Equation (18) and collecting terms, one obtains equations for the wave-like mode and the stationary mode of the EMP.

$$\begin{aligned} &\text{a)}\ \ddot{\boldsymbol{u}}(\boldsymbol{r},t) = \frac{v_s^2 v_\ell^2}{v_\ell^2 + v_s^2}\left\{\nabla\left[\nabla\bullet\boldsymbol{u}(\boldsymbol{r},t)\right] - \nabla\times\nabla\times\boldsymbol{u}(\boldsymbol{r},t)\right\} + \hat{\boldsymbol{a}}_\alpha g\frac{\partial h}{\partial u_\alpha} \quad \text{wave mode} \\ &\text{b)}\ 0 = v_\ell^2\nabla\left[\nabla\bullet\boldsymbol{s}(\boldsymbol{r})\right] - v_s^2\nabla\times\nabla\times\boldsymbol{s}(\boldsymbol{r}) \quad \text{stationary mode} \end{aligned} \tag{21}$$

The wave-like mode of the EMPs is similar to the orbital mode, and the stationary mode of the EMPs is similar to the center of mass mode of an orbiting system. Defining the velocity v_c:

$$v_c^2 \equiv \frac{v_s^2 v_\ell^2}{v_s^2 + v_\ell^2} \tag{22}$$

where v_c = 3187.198854 m per second.

Proceeding with the calculation of the wave-like mode of Equation (21a). In Cylindrical coordinates, only the wave equation for the z direction coordinate is independent. The wave equations for the two perpendicular displacement components are coupled. The gravity force in the horizontal fiber is in the down direction. Therefore, the gravity force has no z direction component. Substituting Equations (22) and (B4) of **Appendix B** for the z displacement component into Equation (21a).

$$\ddot{u}_z = v_c^2\left[\frac{1}{r}\frac{\partial u_z}{\partial r} + \frac{\partial^2 u_z}{\partial r^2} + \frac{1}{r^2}\frac{\partial^2 u_z}{\partial\theta^2} + \frac{\partial^2 u_z}{\partial z^2}\right] \tag{23}$$

We hypothesize that the displacement components were in the form of waves:

$$u_z = U_z(r)\cos\theta\exp(j\omega t - jkz) \tag{24}$$

In the θ direction this mode has a standing wave. Substituting Equation (24) into Equation (23)

$$\begin{aligned} &\text{a)}\ -\omega^2 U_z(r) = v_c^2\left[\frac{1}{r}\frac{\partial U_z(r)}{\partial r} + \frac{\partial^2 U_z(r)}{\partial r^2} - \frac{1}{r^2}U_z(r) - k^2 U_z(r)\right] \\ &\text{b)}\ \frac{1}{r}\frac{\partial U_z(r)}{\partial r} + \frac{\partial^2 U_z(r)}{\partial r^2} - \frac{1}{r^2}U_z(r) + \left(\frac{\omega^2}{v_c^2} - k^2\right)U_z(r) = 0 \end{aligned} \tag{25}$$

Defining the radial wave vector w_z for the z displacement component.

$$w_z^2 \equiv k^2 - \frac{\omega^2}{v_c^2} \tag{26}$$

Substituting Equation (26) into Equation (25b) and dividing the resulting Equation by w_z^2.

$$\frac{1}{w_z r}\frac{\partial U_z\left(w_z r\right)}{\partial\left(w_z r\right)}+\frac{\partial^2 U_z\left(w_z r\right)}{\partial\left(w_z r\right)^2}-\left[\frac{1}{\left(w_z r\right)^2}+1\right]U_z\left(w_z r\right)=0 \tag{27}$$

Equation (27) is a Bessel equation with solutions of a Modified Bessel Function of the second kind of order 1, $K_1\left(w_z r\right)$ in this cylindrically symmetric system.

$$U_z\left(w_z r\right)=B_z K_1\left(w_z r\right) \tag{28}$$

where B_z is an Amplitude constant.

Returning to the wave equation of the r and θ displacement components. Substituting Equations (22) and (B4) of **Appendix B**, into Equation (21a) to obtain a wave equation for the r displacement component.

$$\ddot{u}_r=v_c^2\left[\frac{1}{r}\frac{\partial u_r}{\partial r}+\frac{\partial^2 u_r}{\partial r^2}-\frac{u_r}{r^2}-\frac{2}{r^2}\frac{\partial u_\theta}{\partial\theta}+\frac{1}{r^2}\frac{\partial^2 u_r}{\partial\theta^2}+\frac{\partial^2 u_r}{\partial z^2}\right]+g\frac{\partial h}{\partial u_r} \tag{29}$$

where $g\dfrac{\partial h}{\partial u_r}$ is the gravitational force component per unit mass in the r displacement direction. Substituting Equations (22) and (B4) of **Appendix B** into Equation (21a) for the θ displacement component. Similar to Equation (29) but with the gravity force component per unit mass $g\dfrac{\partial h}{\partial u_\theta}$ in the θ direction.

$$\ddot{u}_\theta=v_c^2\left[\frac{1}{r}\frac{\partial u_\theta}{\partial r}+\frac{\partial^2 u_\theta}{\partial r^2}-\frac{u_\theta}{r^2}+\frac{1}{r^2}\frac{\partial^2 u_\theta}{\partial\theta^2}+\frac{\partial^2 u_\theta}{\partial z^2}+\frac{2}{r^2}\frac{\partial u_r}{\partial\theta}\right]+g\frac{\partial h}{\partial u_\theta} \tag{30}$$

Similar to Equation (29) $g\dfrac{\partial h}{\partial u_\theta}$ is the gravity force component per unit mass in the direction of the θ displacement. We hypothesize that the displacement components were in the form of waves, but the transverse displacement components have the same angular dependence as the gravitational effect on the horizontal fiber:

$$\begin{aligned}&\text{a)}\ u_r=U_r\cos\theta\exp\left(j\omega t-jkz\right)\\&\text{b)}\ u_\theta=U_\theta\sin\theta\exp\left(j\omega t-jkz\right)\end{aligned} \tag{31}$$

As described in the introduction, the EMP move in loops in the CISAW and the gravity components in the direction of the motion of the EMP's have the same wave form as the displacement components. The gravity components act on the EMP's.

$$\begin{aligned}&\text{a)}\ g\frac{\partial h}{\partial u_r}=gG_r\left(r\right)\cos\theta\exp\left(j\omega t-jkz\right)\\&\text{b)}\ g\frac{\partial h}{\partial u_\theta}=gG_\theta\left(r\right)\sin\theta\exp\left(j\omega t-jkz\right)\end{aligned} \tag{32}$$

Therefore, the gravity functions G_r and G_θ are dimensionless parameters that have the same r functional form as the r and θ displacement components. Here U_r and U_θ, are radial coordinate dependent r and θ displacement amplitudes. Substituting Equations (31) and (32) into Equations (29) and (30).

$$\begin{aligned}
\text{a)}\ -\omega^2 U_r\cos\theta &= v_c^2\left[\frac{1}{r}\frac{\partial U_r}{\partial r}+\frac{\partial^2 U_r}{\partial r^2}-\frac{2U_r}{r^2}-k^2U_r\right]\cos\theta \\
&\quad + gG_r\cos\theta - jv_c^2\frac{2}{r^2}U_\theta\cos\theta \\
\text{b)}\ -\omega^2 U_\theta\sin\theta &= v_c^2\left[\frac{1}{r}\frac{\partial u_\theta}{\partial r}+\frac{\partial^2 u_\theta}{\partial r^2}-\frac{2U_\theta}{r^2}-k^2U_\theta\right]\sin\theta \\
&\quad + gG_\theta\sin\theta - jv_c^2\frac{2}{r^2}U_r\sin\theta
\end{aligned} \tag{33}$$

where in Equation (33a) $\cos\theta$ was cancelled and in Equation (33b) $\sin\theta$ was cancelled. Dividing Equations (33) by v_c^2 and collecting terms.

$$\begin{aligned}
\text{a)}\ 0 &= \frac{1}{r}\frac{\partial U_r}{\partial r}+\frac{\partial^2 U_r}{\partial r^2}-\frac{2U_r}{r^2}+\left(\frac{\omega^2}{v_c^2}-k^2\right)U_r+\frac{gG_r}{v_c^2}-j\frac{2}{r^2}U_\theta \\
\text{b)}\ 0 &= \frac{1}{r}\frac{\partial U_\theta}{\partial r}+\frac{\partial^2 U_\theta}{\partial r^2}-\frac{2U_\theta}{r^2}+\left(\frac{\omega^2}{v_c^2}-k^2\right)U_\theta+\frac{gG_\theta}{v_c^2}-j\frac{2}{r^2}U_r
\end{aligned} \tag{34}$$

Assuming one can express the functions $U_r(r)$, $U_\theta(r)$, $G_r(r)$, and $G_\theta(r)$, in as yet not defined functions $P_r(r)$ and $P_\theta(r)$ of the r coordinate multiplied by constants.

$$\begin{aligned}
&\text{a)}\ U_r = B_rP_r(r) && \text{b)}\ U_\theta = B_\theta P_\theta(r) \\
&\text{c)}\ G_r \equiv \frac{B_r}{\gamma_r}P_r(r) && \text{d)}\ G_\theta \equiv \frac{B_\theta}{\gamma_\theta}P_\theta(r)
\end{aligned} \tag{35}$$

where $P_r(r)$ and $P_\theta(r)$ are as of yet not specified functions of r and B_r and B_θ are constants. Here γ_r and γ_θ are gravity effect length associated with the displacement Amplitudes as described in the Introduction. Substituting Equation (35) into Equation (34).

$$\begin{aligned}
\text{a)}\ 0 &= \left[\frac{1}{r}\frac{\partial P_r}{\partial r}+\frac{\partial^2 P_r}{\partial r^2}-\frac{2P_r}{r^2}+\left(\frac{\omega^2}{v_c^2}-k^2+\frac{g}{\gamma_r v_c^2}\right)P_r\right]B_r - j\frac{2}{r^2}P_\theta B_\theta \\
\text{b)}\ 0 &= \left[\frac{1}{r}\frac{\partial P_\theta}{\partial r}+\frac{\partial^2 P_\theta}{\partial r^2}-\frac{2P_\theta}{r^2}+\left(\frac{\omega^2}{v_c^2}-k^2+\frac{g}{\gamma_\theta v_c^2}\right)P_\theta\right]B_\theta - j\frac{2}{r^2}P_rB_r
\end{aligned} \tag{36}$$

The determinate of Equation (36) must be equal to zero.

$$\begin{aligned}
&-j\frac{2}{r^2}P_r\left[\frac{1}{r}\frac{\partial P_r}{\partial r}+\frac{\partial^2 P_r}{\partial r^2}-\frac{2P_r}{r^2}+\left(\frac{\omega^2}{v_c^2}-k^2+\frac{g}{\gamma_r v_c^2}\right)P_r\right] \\
&+j\frac{2}{r^2}P_\theta\left[\frac{1}{r}\frac{\partial P_\theta}{\partial r}+\frac{\partial^2 P_\theta}{\partial r^2}-\frac{2P_\theta}{r^2}+\left(\frac{\omega^2}{v_c^2}-k^2+\frac{g}{\gamma_\theta v_c^2}\right)P_\theta\right]=0
\end{aligned} \tag{37}$$

Defining the radial wave vectors w_r and w_θ for the r and θ displacement components.

$$\text{a)}\ w_r^2 = k^2-\frac{\omega^2}{v_c^2}-\frac{g}{\gamma_r v_c^2} \qquad \text{b)}\ w_\theta^2 = k^2-\frac{\omega^2}{v_c^2}-\frac{g}{\gamma_\theta v_c^2} \tag{38}$$

If we neglect the small gravitational effects, the two terms of Equation (37)

become equal:

$$P\left[\frac{1}{r}\frac{\partial P}{\partial r}+\frac{\partial^2 P}{\partial r^2}-\frac{2P}{r^2}+\left(\frac{\omega^2}{v_c^2}-k^2\right)P\right]\approx 0 \tag{39}$$

Neglecting the gravity effects, substituting Equation (38) into Equation (39) and dividing the resulting Equation by w^2.

$$P\left\{\frac{1}{wr}\frac{\partial P}{\partial(wr)}\frac{\partial^2 P}{\partial(wr)^2}-\left[\frac{2}{(wr)^2}+1\right]P\right\}\approx 0 \tag{40}$$

Equation (40) has two solutions for P, $P=0$ or P is equal to a Modified Bessel function of the second kind of order 2.

$$\text{a)}\ P_r \approx K_2(w_r r) \qquad \text{b)}\ P_\theta \approx K_2(w_\theta r) \tag{41}$$

where we took the liberty to reintroduce the small gravitational effects. Substituting Equation (41) into Equation (35) and the resulting Equations into Equation (31) we obtain the form of the three displacement components:

$$\begin{aligned}&\text{a)}\ u_r = B_r K_2(w_r r)\cos\theta\exp(j\omega t - jkz)\\ &\text{b)}\ u_\theta = B_\theta K_2(w_\theta r)\sin\theta\exp(j\omega t - jkz)\\ &\text{c)}\ u_z = B_z K_1(w_z r)\cos\theta\exp(j\omega t - jkz)\end{aligned} \tag{42}$$

where w_r and w_θ are given by Equation (38) and Equation (42c) is derived from Equations (24) and (26).

3. Derivation of Boundary Conditions

We hypnotize that we neglected forces due to the air on the inner surface of the tubular fiber at $r=a$, where a is the core radius. The strain components in cylindrical coordinates are given in **Appendix C**. The stress σ_{rr} on the inside surface at $r=a$, must be equal to zero.

$$\begin{aligned}&\text{a)}\ \sigma_{rr}=0\\ &\text{b)}\ (\lambda+\mu)\frac{\partial u_r}{\partial r}\Big]_{r=a}-\lambda\left\{\frac{u_r}{a}+\frac{1}{r}\frac{\partial u_\theta}{\partial\theta}\Big]_{r=a}\right\}-\lambda\frac{\partial u_z}{\partial z}\Big]_{r=a}=0\end{aligned} \tag{43}$$

Substituting Equations (42) into (43) and collecting terms with the same angular dependence.

$$\begin{aligned}&B_r\left\{(\lambda+\mu)w_r\frac{\mathrm{d}K_2(w_r r)}{\mathrm{d}(w_r r)}\Big]_{r=a}-\frac{\lambda}{a}K_2(w_r a)\right\}\cos\theta\\ &-\frac{\lambda}{a}B_\theta K_2(w_\theta a)\cos\theta+j\lambda k B_z K_1(w_z a)\cos\theta=0\end{aligned} \tag{44}$$

Substituting Equation (D1) of **Appendix D** into Equation (44) for the derivative of the Modified Bessel Function of the second kind.

$$B_r\left[-\frac{1}{2}(\lambda+\mu)w_r(K_1+K_3)-\frac{\lambda}{a}K_2\right]-B_\theta\frac{\lambda}{a}K_2+jB_z\lambda k K_1=0 \tag{45}$$

The shear stresses from Equations (C1d) and (C1e) of **Appendix C** on the

inside surface must also be equal to zero at $r = a$.

The symmetrized shear stress component $\sigma_{r\theta}$ represents a force acting in the r direction on a surface that is perpendicular to the θ direction. This is the rz surface. It also represents a force in the θ direction acting on a surface perpendicular to the r direction. This is the $z\theta$ surface.

The symmetrized shear stress component σ_{rz} represents a force acting in the r direction on a surface that is perpendicular to the z direction. This is the $r\theta$ surface. It also represents a force in the z direction on a surface that is perpendicular to the r direction. This is the $z\theta$ surface.

$$\begin{aligned} &\text{a)}\ \sigma_{r\theta} = 0 && \text{b)}\ \sigma_{rz} = 0 \\ &\text{c)}\ \sigma_{r\theta} = \frac{\mu}{2}\left(\frac{\partial u_\theta}{\partial r}\bigg]_{r=a} - \frac{u_\theta}{a} + \frac{1}{a}\frac{\partial u_r}{\partial \theta} \right) && \text{d)}\ \sigma_{rz} = \frac{\mu}{2}\left(\frac{\partial u_r}{\partial z} + \frac{\partial u_z}{\partial r}\bigg]_{r=a} \right) \end{aligned} \tag{46}$$

Substituting Equations (42) into (46) and taking the angular dependences into consideration we obtain:

$$\begin{aligned} &\text{a)}\ \frac{\mu}{2}\left\{ B_\theta w_\theta \frac{\mathrm{d}K_2(w_\theta r)}{\mathrm{d}(w_\theta r)}\bigg]_{r=a} - B_\theta \frac{1}{a}K_2(w_\theta a) - B_r \frac{1}{a}K_2(w_r a) \right\} \sin\theta = 0 \\ &\text{b)}\ \frac{\mu}{2}\left\{ -jkB_r K_2(w_r a) + B_z w_z \frac{\mathrm{d}K_1}{\mathrm{d}(w_z r)}\bigg]_{r=a} \right\} \cos\theta = 0 \end{aligned} \tag{47}$$

Observe from Equation (47b) that the phase of the r displacement component u_r is shifted by 90 degrees with respect to the z displacement component u_z. Observe from Equation (47a) that the amplitudes of the radial displacement u_r and the angular displacement u_θ components are in phase. Therefore, the Energy Momentum packets move in loops that perform a rolling motion in the rz plane and the $z\theta$ plane. Gravity couples to these rolling motions similar to the rolling motion of a looping roller coaster car described in the introduction. The effect of gravity is to slightly distort this rolling motion.

Substituting Equation (D1) for the derivatives of the Modified Bessel Functions of the second kind in Equation (47).

$$\begin{aligned} &\text{a)}\ \frac{\mu}{2}\left[-B_\theta \frac{1}{2}w_\theta (K_1 + K_3) - B_\theta \frac{1}{a}K_2 - B_r \frac{1}{a}K_2 \right] = 0 \\ &\text{b)}\ \frac{\mu}{2}\left[-jkB_r K_2 - B_z \frac{1}{2}w_z (K_0 + K_2) \right] = 0 \end{aligned} \tag{48}$$

Equations (45) and (48) are written in matrix form as follows:

$$\begin{vmatrix} -\frac{1}{2}(\lambda+\mu)w_r(K_1+K_3) - \frac{\lambda}{a}K_2 & -\frac{\lambda}{a}K_2 & j\lambda k K_1 \\ \frac{1}{a}K_2 & \frac{1}{2}w_\theta(K_1+K_3) + \frac{1}{a}K_2 & 0 \\ jkK_2 & 0 & \frac{1}{2}w_z(K_0+K_2) \end{vmatrix} = 0 \tag{49}$$

The determinate of the matrix of Equation (49) must be equal to zero.

$$\begin{aligned}&\frac{1}{8}(\lambda+\mu)w_r w_\theta w_z\left(K_1+K_3\right)^2\left(K_0+K_2\right)+\frac{\lambda}{4a}w_\theta w_z\left(K_1+K_3\right)\left(K_0+K_2\right)K_2\\&+\frac{1}{4a}(\lambda+\mu)w_r w_z\left(K_1+K_3\right)\left(K_0+K_2\right)K_2+\frac{\lambda}{2a^2}w_z\left(K_0+K_2\right)K_2^2\\&-\frac{\lambda}{2a^2}w_z\left(K_0+K_2\right)K_2^2-\frac{1}{2}\lambda k^2 w_\theta\left(K_1+K_3\right)K_1K_2-\lambda\frac{1}{a}k^2K_1K_2^2=0\end{aligned}\tag{50}$$

In order to formalize Equation (50) in dimensionless form we multiply Equation (50) by the constants a^3 and divide by λ.

$$\begin{aligned}&\frac{1}{8}\frac{\lambda+\mu}{\lambda}w_r w_\theta w_z a^3\left(K_1+K_3\right)^2\left(K_0+K_2\right)\\&+\frac{1}{4}w_\theta w_z a^2\left(K_1+K_3\right)\left(K_0+K_2\right)K_2\\&+\frac{1}{4}\frac{\lambda+\mu}{\lambda}a^2 w_r w_z\left(K_1+K_3\right)\left(K_0+K_2\right)K_2\\&-\frac{1}{2}k^2a^3w_\theta\left(K_1+K_3\right)K_1K_2-k^2a^2K_1K_2^2=0\end{aligned}\tag{51}$$

Substituting Equations (26) and (38) for the radial wave vectors w_r, w_θ and w_z into Equation (51) and factoring out k.

$$\begin{aligned}&\frac{\lambda+\mu}{8\lambda}k^3a^3\sqrt{1-\frac{\omega^2}{k^2v_c^2}}\sqrt{1-\frac{\omega^2}{k^2v_c^2}-\frac{g}{k^2\gamma_r v_c^2}}\sqrt{1-\frac{\omega^2}{k^2v_c^2}-\frac{g}{k^2\gamma_\theta v_c^2}}\left(K_1+K_3\right)^2\left(K_0+K_2\right)\\&+\frac{1}{4}k^2a^2\sqrt{1-\frac{\omega^2}{k^2v_c^2}}\sqrt{1-\frac{\omega^2}{k^2v_c^2}-\frac{g}{k^2\gamma_\theta v_c^2}}\left(K_1+K_3\right)\left(K_0+K_2\right)K_2\\&+\frac{1}{4}\frac{\lambda+\mu}{\lambda}k^2a^2\sqrt{1-\frac{\omega^2}{k^2v_c^2}}\sqrt{1-\frac{\omega^2}{k^2v_c^2}-\frac{g}{k^2\gamma_r v_c^2}}\left(K_1+K_3\right)\left(K_0+K_2\right)K_2\\&-\frac{1}{2}k^3a^3\sqrt{1-\frac{\omega^2}{k^2v_c^2}-\frac{g}{k^2\gamma_\theta v_c^2}}\left(K_1+K_3\right)K_1K_2-k^2a^2K_1K_2^2=0\end{aligned}\tag{52}$$

Defining a dimensionless parameter

$$q^2\equiv\frac{\omega^2}{k^2v_c^2}\tag{53}$$

Substituting the parameter q^2 of Equation (53) into Equation (52) and factoring out $1-q^2$.

$$\begin{aligned}&\frac{\lambda+\mu}{8\lambda}k^3a^3\left(1-q^2\right)^{\frac{3}{2}}\sqrt{1-\frac{g}{\gamma_r k^2v_c^2\left(1-q^2\right)}}\sqrt{1-\frac{g}{\left(1-q^2\right)k^2\gamma_\theta v_c^2}}\left(K_1+K_3\right)^2\left(K_0+K_2\right)\\&+\frac{1}{4}k^2a^2\left(1-q^2\right)\sqrt{1-\frac{g}{k^2\gamma_\theta v_c^2\left(1-q^2\right)}}\left(K_1+K_3\right)\left(K_0+K_2\right)K_2\\&+\frac{1}{4}\frac{\lambda+\mu}{\lambda}k^2a^2\left(1-q^2\right)\sqrt{1-\frac{g}{k^2\gamma_r v_c^2\left(1-q^2\right)}}\left(K_1+K_3\right)\left(K_0+K_2\right)K_2\\&-\frac{1}{2}k^3a^3\sqrt{1-q^2}\sqrt{1-\frac{g}{k^2\gamma_\theta v_c^2\left(1-q^2\right)}}\left(K_1+K_3\right)K_1K_2-k^2a^2K_1K_2^2=0\end{aligned}\tag{54}$$

Expanding Equation (54) to lowest order in $\frac{g}{k^2\gamma_r v_c^2\left(1-q^2\right)}$ and $\frac{g}{k^2\gamma_\theta v_c^2\left(1-q^2\right)}$.

$$\begin{aligned}
&\frac{\lambda+\mu}{8\lambda}k^3a^3\left(1-q^2\right)^{\frac{3}{2}}\left[1-\frac{g}{2k^2v_c^2\left(1-q^2\right)}\left(\frac{1}{\gamma_r}+\frac{1}{\gamma_r}\right)\right]\left(K_1+K_3\right)^2\left(K_0+K_2\right)\\
&+\frac{1}{4}k^2a^2\left(1-q^2\right)\left[1-\frac{g}{2k^2\gamma_\theta v_c^2\left(1-q^2\right)}\right]\left(K_1+K_3\right)\left(K_0+K_2\right)K_2\\
&+\frac{1}{4}\frac{\lambda+\mu}{\lambda}k^2a^2\left(1-q^2\right)\left[1-\frac{g}{2k^2\gamma_r v_c^2\left(1-q^2\right)}\right]\left(K_1+K_3\right)\left(K_0+K_2\right)K_2\\
&-\frac{1}{2}k^3a^3\sqrt{1-q^2}\left[1-\frac{g}{2k^2\gamma_\theta v_c^2\left(1-q^2\right)}\right]\left(K_1+K_3\right)K_1K_2-k^2a^2K_1K_2^2=0
\end{aligned}\tag{55}$$

The CISAW mode can be calculated by neglecting the small gravity term in Equation (55). For this case all transverse wave vectors w_r, w_θ, and w_z are equal and the argument x of the Modified Bessel Functions of the second kind are:

$$\text{a)}\ K_\eta=K_\eta\left(x\right)\qquad \text{b)}\ x\equiv aw\qquad \text{c)}\ x=ka\sqrt{1-q^2}\tag{56}$$

Neglecting the small effect of gravity and substituting Equation (56) into Equation (55) to calculate the first order angular standing wave CISAW mode.

$$\begin{aligned}
&\text{a)}\ \xi=0\\
&\text{b)}\ \xi=\frac{1}{8}\frac{\lambda+\mu}{\lambda}x^3\left(K_1+K_3\right)^2\left(K_0+K_2\right)\\
&\quad+\frac{1}{4}\left(\frac{\lambda+\mu}{\lambda}+1\right)x^2\left(K_1+K_3\right)\left(K_0+K_2\right)K_2\\
&\quad-\frac{x^3}{2\left(1-q^2\right)}\left(K_1+K_3\right)K_1K_2-\frac{x^2}{1-q^2}K_1K_2^2
\end{aligned}\tag{57}$$

Equation (57) is nonlinear in x because the Modified Bessel Functions of the second kind $K_\eta\left(x\right)$ are functions of x. The asymptotic approximation [20] for the Modified Bessel Functions of the second kind from Equations (D3a) and (D3b) of **Appendix D** are used for the numeric solution of Equation (57). Chipmunk Basic software is used for the numeric calculations.

Equation (57), has one root x for each value of q. These roots x are obtained by calculating ξ from Equation (57) for successive values of x at a fixed value of q until a sufficient small value of $\left|\xi\right|<10^{-6}$ is obtained. The value of x giving the smallest value of ξ is the root x of Equation (57).

At this point in the calculation, Lord Rayleigh [1] obtained a cubic equation. His calculation of SAW's on a flat surface involve sin's, cos's, and exponentials, while SAW's propagating on a cylindrical surface involved Modified Bessel Functions of the second kind.

The highly non-linear Equation (57) does not seem to have roots x for values of q less than $q = 0.88$ and more than $q = 0.94$. There are also two ranges of roots x for q between $q = 0.88$ and $q = 0.900016$ and between $q = 0.900016$ and $q = 0.94$. At the boundary of the two ranges at $q = 0.89992$, x has a value of $x = 1.01283$ and at the value of $q = 0.900016$, x has a value of $x = 0.025405$.

The dispersion relation can be calculated from the roots x and the values q of Equation (57). Figure 1 shows a plot of the longitudinal wave vector k as a function of frequency for values of q between $q = 0.900016$ and $q = 0.94$. This is the dispersion relation of the CISAW.

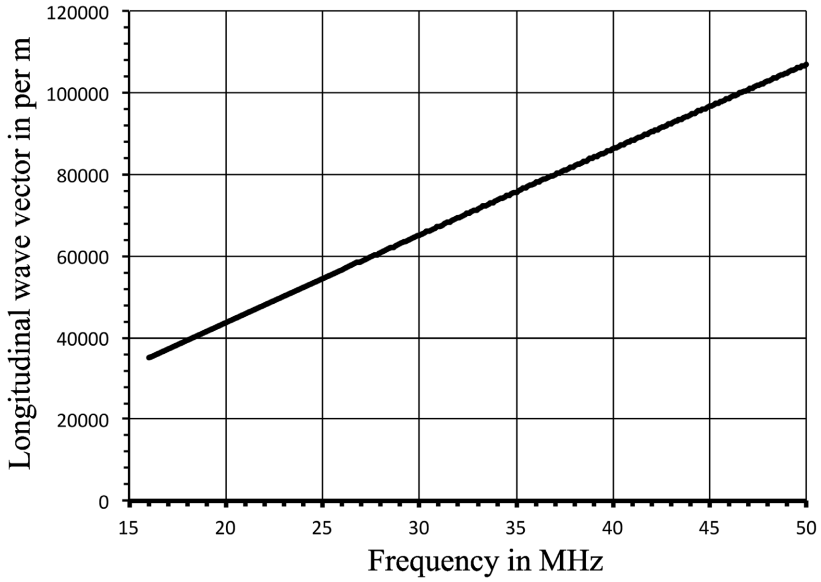

Figure 1. The dispersion relation of the first order angular mode of the CISAW propagating on the inside surface of a simple tubular fused quartz fiber with a core diameter of 12 μm is plotted above. The longitudinal wave vector $k = \frac{2\pi}{\lambda_{CSAW}}$. There are other modes besides the first order angular mode shown here, but only the first order angular mode couples to gravity.

The group velocity v_g is the change of the radial velocity ω with the longitudinal wave vector k.

$$v_g = \frac{\mathrm{d}\omega}{\mathrm{d}k} \tag{58}$$

The group velocity v_g as a function of the frequency is given in Figure 2.

Substituting Equation (56c) for x into Equation (55)

$$\begin{aligned} &\frac{\lambda+\mu}{8\lambda}x^3\left(1-\frac{ga^2}{\gamma v_c^2 x^2}\right)\left(K_1+K_3\right)^2\left(K_0+K_2\right) \\ &+\frac{1}{4}\left(\frac{\lambda+\mu}{\lambda}+1\right)x^2\left(1-\frac{ga^2}{2\gamma v_c^2 x^2}\right)\left(K_1+K_3\right)\left(K_0+K_2\right)K_2 \\ &-\frac{1}{2\left(1-q^2\right)}x^3\left(1-\frac{ga^2}{2\gamma v_c^2 x^2}\right)\left(K_1+K_3\right)K_1K_2-k^2a^2K_1K_2^2=0 \end{aligned} \tag{59}$$

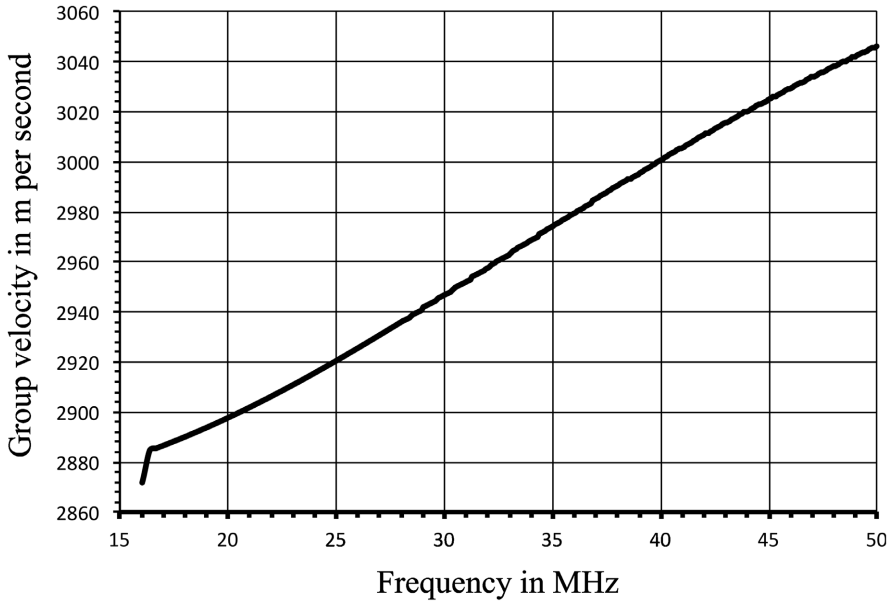

Figure 2. The CISAW group velocity v_g as a function of the frequency for a tubular fiber with a 12 μm core diameter is plotted above. The group velocity at a frequency of 25.081966 MHz is 2920.95615 m per second.

where for simplicity we assumed that $\gamma_\theta = \gamma_r$. In order to calculate the change Δk of the wave vector k we hypothesize that the parameter x consists of x and a small change Δx. That is, $x \to x + \Delta x$ in Equation (59). By multiplying out Equation (59) to lowest order.

$$\begin{aligned}
&\frac{\lambda+\mu}{8\lambda}\left(x^3+3x^2\Delta x-\frac{ga^2}{\gamma v_c^2}x\right)\left(K_1+K_3\right)^2\left(K_0+K_2\right)\\
&+\frac{\lambda+\mu}{4\lambda}w\left(K_1+K_3\right)\left(K_0+K_2\right)\left[\frac{\mathrm{d}K_1}{\mathrm{d}(wr)}+\frac{\mathrm{d}K_3}{\mathrm{d}(wr)}\right]_{r=a}\Delta x+\cdots\\
&+\frac{1}{4}\left(\frac{\lambda+\mu}{\lambda}+1\right)\left(x^2+2x\Delta x-\frac{ga^2}{2\gamma v_c^2}\right)\left(K_1+K_3\right)\left(K_0+K_2\right)K_2\\
&-\frac{1}{2\left(1-q^2\right)}\left(x^3+3x^2\Delta x-\frac{ga^2}{2\gamma v_c^2}x\right)\left(K_1+K_3\right)K_1K_2-k^2a^2K_1K_2^2=0
\end{aligned} \tag{60}$$

Substituting Equation (57) into Equation (60) and for simplicity neglecting the expansions of the Modified Bessel Functions of the second kind in Δx one obtains:

$$\begin{aligned}
&\frac{\lambda+\mu}{8\lambda}\left(3x^2\Delta x-\frac{ga^2}{\gamma v_c^2}x\right)\left(K_1+K_3\right)^2\left(K_0+K_2\right)\\
&+\frac{1}{4}\left(\frac{\lambda+\mu}{\lambda}+1\right)\left(2x\Delta x-\frac{ga^2}{2\gamma v_c^2}\right)\left(K_1+K_3\right)\left(K_0+K_2\right)K_2\\
&-\frac{1}{2\left(1-q^2\right)}\left(3x^2\Delta x-\frac{ga^2}{2\gamma v_c^2}x\right)\left(K_1+K_3\right)K_1K_2=0
\end{aligned} \tag{61}$$

One can solve Equation (61) for Δx

$$\Delta x = \frac{ga^2}{2\gamma v_c^2}\left[\frac{\lambda+\mu}{4\lambda}x\left(K_1+K_3\right)^2\left(K_0+K_2\right)\right.$$
$$+\frac{1}{4}\left(\frac{\lambda+\mu}{\lambda}+1\right)\left(K_1+K_3\right)\left(K_0+K_2\right)K_2$$
$$\left.-\frac{x}{2\left(1-q^2\right)}\left(K_1+K_3\right)K_1K_2\right]\left[\frac{3(\lambda+\mu)}{8\lambda}x^2\left(K_1+K_3\right)^2\left(K_0+K_2\right)\right. \tag{62}$$
$$\left.+\frac{1}{2}\left(\frac{\lambda+\mu}{\lambda}+1\right)x\left(K_1+K_3\right)\left(K_0+K_2\right)K_2-\frac{3x^2}{2\left(1-q^2\right)}\left(K_1+K_3\right)K_1K_2\right]^{-1}$$

Similar to Equation (56c)

$$\Delta x \approx \Delta ka\sqrt{1-q^2} \tag{63}$$

Substituting Equation (63) into Equation (62) and solving for Δk.

$$\Delta k = \frac{ga}{2\gamma v_c^2\sqrt{1-q^2}}\left[\frac{\lambda+\mu}{4\lambda}x\left(K_1+K_3\right)^2\left(K_0+K_2\right)\right.$$
$$+\frac{1}{4}\left(\frac{\lambda+\mu}{\lambda}+1\right)\left(K_1+K_3\right)\left(K_0+K_2\right)K_2$$
$$\left.-\frac{x}{2\left(1-q^2\right)}\left(K_1+K_3\right)K_1K_2\right]\left[\frac{3(\lambda+\mu)}{8\lambda}x^2\left(K_1+K_3\right)^2\left(K_0+K_2\right)\right. \tag{64}$$
$$\left.+\frac{1}{2}\left(\frac{\lambda+\mu}{\lambda}+1\right)x\left(K_1+K_3\right)\left(K_0+K_2\right)K_2-\frac{3x^2}{2\left(1-q^2\right)}\left(K_1+K_3\right)K_1K_2\right]^{-1}$$

The values of x, q, and the Modified Bessel Functions of the second kind are

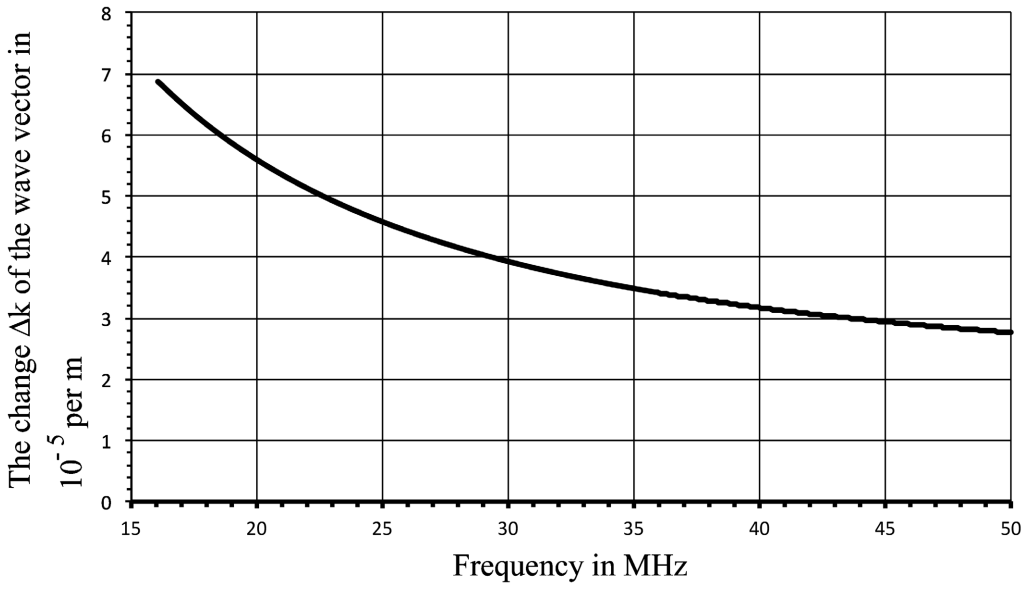

Figure 3. The change Δk of the longitudinal wave vector with gravity of the CISAW in units of 10^{-5} per m is plotted above. At a frequency of 25.081966 MHz the change Δk of the wave vector has a value of 4.562951×10^{-5} per m. This change Δk of the CISAW wave vector due to gravity is 35073 times as large as the change $\Delta ß$ of a light beam wave vector due to gravity.

calculated from Equation (57b). A plot of the change Δk of the wave vector with gravity as a function of frequency is shown in Figure 3.

4. Conclusion and Discussion

The modes of Surface Acoustic Waves propagating on the inside surface of a horizontal tubular high purity fused quartz fiber with an inside diameter of 12 μm, and the change in the wave vector due to gravity, of this wave was investigated in this study.

4.1. Energy Momentum Packet Modes

In the Classical Continuum Mechanics model used here, an infinitesimal mass consists of a sufficient number of atoms to be considered as a continuum. In an elastic wave in a solid, infinitesimal masses only move less than an infinitesimal distance. Each infinitesimal mass bumps against the next infinitesimal mass etc. This slightly compresses the infinitesimal mass. In each collision it transfers Kinetic Energy and Momentum, and when it re-expands it also transfers Elastic Potential Energy to the next infinitesimal mass. Therefore, in an elastic wave in a solid, Energy Momentum Packets (EMP), not infinitesimal masses, propagate along the elastic wave [3]. The EMP's have mass.

Ocean Waves [3] similar to SAW's have a rolling motion. In Ocean Waves Infinitesimal water volumes do not move in a rolling motion, only Energy Momentum packets move in a rolling motion. An example is that boats similar to infinitesimal masses are not dragged along by a wave, nor are they pulled under as the rolling Ocean Wave passes, but just bob up and down.

The EMP's in a CISAW propagating on the inside surface of a horizontal tubular fiber experiences two restoring forces, an elastic restoring force and a much smaller gravitational restoring force. The gravitational restoring force on EMP's of CISAW's are similar to the restoring force on EMP's of deep-ocean surface waves.

To my knowledge, this is the first publication to date (2024) reporting Acoustic Surface Waves (SAW) propagating on the inside surface of a tube.

4.2. Surface Acoustic Waves and Boundary Conditions

There were a lot of publications on SAW propagating on flat surfaces. SAW devices with the SAW propagating on piezoelectric LiNbO3 crystal wafers are used to process electronic signals. There are SAW light deflectors. There was a Camera that produced the two-dimensional Fourier Transform of the image light intensity using SAW's [5]. But in all these devices the SAW's propagated on flat surfaces. Lord Rayleigh [1] published the first analysis of SAW's on flat surfaces.

Lord Rayleigh postulated a wave formulism to derive the SAW wave equation. His derivation did not start from the general anisotropic elastic properties of solids. In this study the CISAW's are derived from basic principles starting with the derivation of the elastic potential energy density. Using this elastic potential

energy density, the CISAW wave equation was derived by a variational principle similar to the one used for deriving the Euler Lagrange equations.

The force on the inside surface of the fiber is zero if the effect of air is neglected. The requirement that the force on the inside surface of the tubular fiber is zero, couples the longitudinal and shear elastic motions. This coupled motion produces Surface Wave modes with EMP's moving in loops as they propagate along the fiber inside surface.

4.3. Effect of Gravity

The Newtonian model of gravity is used in this study. The effect of gravity on the EMP is similar to the effect of gravity on a pendulum bob. The explanation of this effect is as follows: The path of the pendulum is determined by the fixed length pendulum arm. The component of the gravity force on the pendulum bob along its motion changes with the direction of the pendulum bob motion. The gravity force component along the pendulum bob motion changes from a value of zero when the pendulum is moving horizontally at the bottom of its motion to a non-zero value when the pendulum bob moves at an angle to the horizontal direction. The pendulum bob moves down due to the gravity force. At the bottom when the pendulum moves horizontally the gravity force is equal to zero. But at this point the gravity potential energy was transferred to kinetic energy and the pendulum moves up against a gravity force component until it lost its kinetic energy. At the top of the pendulum bob motion gravity again takes over making the pendulum swing down.

The looping path of the EMP is determined by its inertia and the elastic restoring force it experiences. The effect of gravity on the mass of EMP is similar to the effect of gravity on a pendulum bob. The component of gravity in the direction of the EMP motion also changes as the EMP moves in a loop. At the top and bottom of the loop where the EMP move horizontally the component of the gravity force along the EMP path is zero, and when the EMP moves vertically in the loop the gravity force component along its path is a maximum. Thus the gravity force component along the EMP path is also a wave with the same frequency and wavelength as the CISAW. Thus gravity couples to CISAW's. The effect of space-time on the EMP is much smaller than the Newtonian effect of gravity described here. It is left to future scientists to calculate the effect of the curvature of space-time on CISAW's.

There could be other elastic modes where the EMP motion is not just horizontal or vertical such as in Torsional Elastic Waves where a component of the Newtonian gravity force could couple to the EMP motion. This is for other scientists to investigate.

In this study the effect of Earth gravity on the propagation of CISAW was derived. In the future this should be re-derived for arbitrary gravitational fields such as the gravity fields associated with gravity waves.

4.4. Results

The dispersion relation for the CISAW are calculated from highly non linear equations involving modified Bessel Functions of the second kind. In systems

with rectangular symmetry the exponentials, sins and cosines cancel. However, however for the CISAW the modified Bessel Functions of the second kind do not cancel. The results of this papers calculations are: at a frequency of 25.081966 MHz the change Δk of the wave vector due to the effect of gravity is 4.562951×10^{-5} per m. This is 35073 times as large as the change in wave vector $\Delta ß = 1.301 \times 10^{-9}$ per m with gravity calculated for a light wave propagating in an optical fiber [21]. At the same frequency less than −60 dB of the displacement amplitude reaches the outside of the fiber if it has an outside diameter of at least 221.949 μm. By comparison the outside diameter of a single mode optical fiber is 125 μm. At a frequency of 25.081966 MHz the group velocity of a CISAW is 2920.95615 m per second, and at the same frequency, the wave vector k is equal to $\frac{2\pi}{\lambda_{CSAW}} =$ 54,678.0572 per m. The dispersion relation is shown in **Figure 1**.

4.5. Suggested Future Work

First, high purity fused quartz tubular fibers should be fabricated. Next, the transmission properties of CISAW propagating on the inside surface of these tubular fibers calculated in this study need to be measured experimentally. The propagation losses of the CISAW also have to be measured. Fiber couplers for the CISAW, similar to couplers for optical fibers, should be developed.

Then the effect of Earth gravity on the propagation parameters of CISAW should be measured. This can be done by measuring the propagation properties of CISAW in tubular fibers at different elevations.

Next, a CISAW interferometer using fiber couplers instead of beam splitters and mirrors need to be designed, built and tested. The construction of the CISAW fiber interferometer is similar to a light fiber interferometer.

Eventually, a gravity measuring CISAW Interferometer should be designed, constructed and tested first using Earth Gravity. Observe if such an interferometer can detect gravity waves. Finally, construct an array of CISAW based gravity wave sensing Interferometers to detect gravity wave images. These would be Sub-Wavelength images since the gravity wavelength is much larger than the spacing between array elements.

There are many other applications of CISAW propagating on the inside surface of a tubular fused quartz fiber such as an Acoustic Endoscope which is impervious to body fluids. The CISAW propagating on the inside surface of a tubular fused quartz fiber can also be used in long delay signal processors.

4.6. Impact on Science

The group velocity of CISAW's is much smaller than the velocity of light and the effect of gravity on the wave vector of CISAW's is much larger than the effect of gravity on the wave vector of light. Therefore, CISAW based gravity detectors would be much smaller than the present km-sized gravity detecting Light Interferometer Gravity-wave Observatory (LIGO) experiment [9], Fiber couplers for CISAW

similar to couplers in optical fibers can be used instead of beam splitters and mirrors. Since the wavelength of gravity waves are much larger than the spacing between CISAW based detector interferometer array elements, the detection would be sub-wavelength imaging [17].

The Fabre Perot cavity with a 4 km space between mirrors in the LIGO experiment bounces the light beam 300 times in an interferometer arm. Light traveling at the speed of light takes 4.00277 milliseconds to travel through the Fabre Perot structure.

CISAW's traveling at a group velocity of 2920.95615 m per second, can traversed an 8 m diameter 50 turn CISAW fiber coil in 0.430214 seconds. This is 107.479 times longer than light traversing a Fabre-Perot cavity in an LIGO arm. Since the outside diameter of the CISAW fiber is 222 micro meters, the 50 turn coil would be 11.1 mm long.

The thin-piezoelectric-film Acoustic Surface Wave Transducers in the fiber ends used for both generating and detecting the CISAW produce very little noise compared to the lasers used in the LIGO [9] experiment. The loss mechanisms in CISAW are similar to the losses in high purity fused quartz optical fibers. There are also losses due to nonlinear elastic effects. There are losses owing to the coupling of elastic waves to the air, however, the hollow core of the tubular fiber can be evacuated reducing the air losses. *It is left to future Scientists to construct gravity wave detecting interferometers using the information derived in this paper.*

An array of CISAW interferometers could for the first time perform gravity wave imaging. This can have a large effect on astronomical observations. It is interesting what future discoveries could be made with a gravity wave imaging system.

Acknowledgments

I thank my wife Marlene Danzig-Kornreich for her suggestions on the text, and for making this paper more understandable to the readers. I also thank her for editing, proofreading, and working together on this manuscript.

Conflicts of Interest

The author declares no conflicts of interest regarding the publication of this paper.

References

[1] Rayleigh, L. (1885) On Waves Propagated along the Plane Surface of an Elastic Solid. *Proceedings of the London Mathematical Society*, **1**, 4-11. https://doi.org/10.1112/plms/s1-17.1.4

[2] Lamb, H. (1889) On the Flexure of an Elastic Plate. *Proceedings of the London Mathematical Society*, **21**, 70-91.

[3] Montanaki, A. (2017) Mechanics of Seawaves. http://www.albertomontanari.il

[4] Wang, W., Liu, J., Xie, X., Liu, M. and He, S. (2011) Development of a New Surface Acoustic Wave Based Gyroscope on a X-112°Y $LiTaO_3$ Substrate. *Sensors*, **11**, 10894-10906. https://doi.org/10.3390/s111110894

[5] Kornreich, P.G., Kowel, S.T., Fleming, D.J., Yang, N.T., Gupta, A. and Lewis, O.

(1974) DEFT: Direct Electronic Fourier Transforms of Optical Images. *Proceedings of the IEEE*, **62**, 1072-1087. https://doi.org/10.1109/proc.1974.9571

[6] Bunney, R.E., Goodman, R.R. and Marshall, S.W. (1969) Rayleigh and Lamb Waves on Cylinders. *The Journal of the Acoustical Society of America*, **46**, 1223-1233. https://doi.org/10.1121/1.1911844

[7] Gazis, D.C. (1959) Three-Dimensional Investigation of the Propagation of Waves in Hollow Circular Cylinders. I. Analytical Foundation. *The Journal of the Acoustical Society of America*, **31**, 568-573. https://doi.org/10.1121/1.1907753

[8] Gazis, D.C. (1959) Three-dimensional Investigation of the Propagation of Waves in Hollow Circular Cylinders. II. Numerical Results. *The Journal of the Acoustical Society of America*, **31**, 573-578. https://doi.org/10.1121/1.1907754

[9] Abbott, B.P., *et al.* (2016) Observation of Gravitational Waves from a Binary Black Hole Merger. *Physical Review Letters*, **116**, Article ID: 061102.

[10] Abbott, R., Abbott, T.D., Abraham, S., *et al.* (2021) Observation of Gravitational Waves from Two Neutron Star-Black Hole Coalescences. *Astrophysics Journal Letters*, **915**, 1-24.

[11] Abbott, R., Abbott, T.D., Abraham, S., *et al.* (2020) Gravitational Waves from the Coalescence of a 23M Black Hole with a 2.6M Compact Object. *Astrophysical Journal Letters*, **896**, 1-30.

[12] Abbott, R., *et al.* (2020) A Binary Black Hole Merger with a Total Mass of 150 $M_{\odot}$. *Physical Review Letters*, **125**, 101102-1-110102-17.

[13] Abbott, R., Abbott, T.D., Abraham, S., *et al.* (2020) Properties and Astrophysical Implications of the 150 $M_{\odot}$ Binary Black Hole Merger. *Astrophysical Journal Letters*, **900**, 1-39.

[14] Abbott, R., Abbott, T.D., Abraham, S., *et al.* (2020) Observation of a Compact Binary Coalescence with Total Mass ~ 3.4 $M_{\odot}$. *Astrophysical Journal Letters*, **892**, 1-24.

[15] Abbott, R., *et al.* (2020) Observation of a Binary-Black-Hole Coalescence with Asymmetric Masses. *Physical Review D*, **102**, 043015-1-043015-29.

[16] Abbott, B.P., *et al.* (2017) A Three-Detector Observation of Gravitational Waves from a Binary Black Hole Coalescence. *Physical Review Letters*, **119**, 141101-1-141101-16.

[17] Neice, A. (2010) Methods and Limitations of Subwavelength Imaging. *Advances in Imaging and Electron Physics*, **163**, 117-140. https://doi.org/10.1016/s1076-5670(10)63003-0

[18] Feynman, R., Leighton, R. and Sands, M. (2020) The Feynman Lectures of Physics. Basic Books Hachette Book Group.

[19] Stratton, J.A. (1941) Formulas from Vector Analysis. *Electromagnetic Theory*, McGraw-Hill Book, 604.

[20] Yang, Z.H. and Chu, Y.M. (2017) On Approximating the Modified Bessel Function of the Second Kind. *Journal of Inequalities and Applications*, **2017**, Article No. 41. https://doi.org/10.1186/s13660-017-1317-z

[21] Beig, R., Chruściel, P.T., Hilweg, C., Kornreich, P. and Walther, P. (2018) Weakly Gravitating Isotropic Waveguides. *Classical and Quantum Gravity*, **35**, Article ID: 244001. https://doi.org/10.1088/1361-6382/aae873

Appendix A

Performing the variation of Equation (6).

$$\begin{aligned}\delta\mathcal{I} = {} & \rho\int_{\tau_b}^{\tau_b}\frac{\mathrm{d}u_a}{\mathrm{d}t}\frac{\delta\mathrm{d}u_a}{\delta\xi\mathrm{d}t}\mathrm{d}t \\ & -\frac{1}{2}c_{\alpha\beta\gamma\delta}\int_{s_a}^{s_b}\left[\frac{\delta\partial u_\alpha}{\delta\xi\partial x_\beta}\frac{\partial u_\gamma}{\partial x_\delta}+\frac{\partial u_\alpha}{\partial x_\beta}\frac{\delta\partial u_\gamma}{\delta\xi\partial x_\delta}+\frac{\delta\partial u_\beta}{\delta\xi\partial x_\alpha}\frac{\partial u_\gamma}{\partial x_\delta}+\frac{\partial u_\beta}{\partial x_\alpha}\frac{\delta\partial u_\gamma}{\delta\xi\partial x_\delta}\right. \\ & \left.+\frac{\delta\partial u_\alpha}{\delta\xi\partial x_\beta}\frac{\partial u_\delta}{\partial x_\gamma}+\frac{\partial u_\alpha}{\partial x_\beta}\frac{\delta\partial u_\delta}{\delta\xi\partial x_\gamma}+\frac{\delta\partial u_\beta}{\delta\xi\partial x_\alpha}\frac{\partial u_\delta}{\partial x_\gamma}+\frac{\partial u_\beta}{\partial x_\alpha}\frac{\delta\partial u_\delta}{\delta\xi\partial x_\gamma}+\rho g\delta_{2\alpha}\frac{\delta u_\alpha}{\delta\xi}\right]\mathrm{d}v\end{aligned} \tag{A1}$$

where $\delta_{2\alpha}$ is a direction cosine not a constant delta function. All except the last terms of Equation (A1), must be integrated by parts. Expanding the first term of Equation (A1).

$$\frac{\mathrm{d}}{\mathrm{d}t}\left[\frac{\mathrm{d}u_\alpha}{\mathrm{d}t}\frac{\delta u_\alpha}{\delta\xi}\right]-\frac{\delta u_\alpha}{\delta\xi}\frac{\mathrm{d}^2u_\alpha}{\mathrm{d}t^2}=\frac{\mathrm{d}\delta u_\alpha}{\mathrm{d}t\delta\xi}\frac{\mathrm{d}u_\alpha}{\mathrm{d}t} \tag{A2}$$

Expanding the 2nd term of Equation (A1)

$$\frac{\partial}{\partial x_\beta}\left[\frac{\delta u_\alpha}{\delta\xi}\frac{\partial u_\gamma}{\partial x_\delta}\right]-\frac{\delta u_\alpha}{\delta\xi}\frac{\partial^2u_\gamma}{\partial x_\beta\partial x_\delta}=\frac{\delta\partial u_\alpha}{\delta\xi\partial x_\beta}\frac{\partial u_\gamma}{\partial x_\delta} \tag{A3}$$

Expanding the 3rd term of Equation (A1)

$$\frac{\partial}{\partial x_\delta}\left[\frac{\partial u_\alpha}{\partial x_\beta}\frac{\delta u_\gamma}{\delta\xi}\right]-\frac{\partial^2u_\alpha}{\partial x_\delta\partial x_\beta}\frac{\delta u_\gamma}{\delta\xi}=\frac{\partial u_\alpha}{\partial x_\beta}\frac{\partial\delta u_\gamma}{\partial x_\delta\delta\xi} \tag{A4}$$

Expanding the 4th term of Equation (A1)

$$\frac{\partial}{\partial x_\alpha}\left[\frac{\delta u_\beta}{\delta\xi}\frac{\partial u_\gamma}{\partial x_\delta}\right]-\frac{\delta u_\beta}{\delta\xi}\frac{\partial^2u_\gamma}{\partial x_\alpha\partial x_\delta}=\frac{\partial\delta u_\beta}{\partial x_\alpha\delta\xi}\frac{\partial u_\gamma}{\partial x_\delta} \tag{A5}$$

Expanding the 5th term of Equation (A1)

$$\frac{\partial}{\partial x_\delta}\left[\frac{\partial u_\beta}{\partial x_\alpha}\frac{\delta u_\gamma}{\delta\xi}\right]-\frac{\partial^2u_\beta}{\partial x_\delta\partial x_\alpha}\frac{\delta u_\gamma}{\delta\xi}=\frac{\partial u_\beta}{\partial x_\alpha}\frac{\partial\delta u_\gamma}{\partial x_\delta\delta\xi} \tag{A6}$$

Expanding the 6th term of Equation (A1)

$$\frac{\partial}{\partial x_\beta}\left[\frac{\delta u_\alpha}{\delta\xi}\frac{\partial u_\delta}{\partial x_\gamma}\right]-\frac{\delta u_\alpha}{\delta\xi}\frac{\partial^2u_\delta}{\partial x_\beta\partial x_\gamma}=\frac{\partial\delta u_\alpha}{\partial x_\beta\delta\xi}\frac{\partial u_\delta}{\partial x_\gamma} \tag{A7}$$

Expanding the 7th term of Equation (A1)

$$\frac{\partial}{\partial x_\gamma}\left[\frac{\partial u_\alpha}{\partial x_\beta}\frac{\delta u_\delta}{\delta\xi}\right]-\frac{\partial^2u_\alpha}{\partial x_\gamma\partial x_\beta}\frac{\delta u_\delta}{\delta\xi}=\frac{\partial u_\alpha}{\partial x_\beta}\frac{\partial\delta u_\delta}{\partial x_\gamma\delta\xi} \tag{A8}$$

Expanding the 8th term of Equation (A1)

$$\frac{\partial}{\partial x_\alpha}\left[\frac{\delta u_\beta}{\delta\xi}\frac{\partial u_\delta}{\partial x_\gamma}\right]-\frac{\delta u_\beta}{\delta\xi}\frac{\partial^2 u_\delta}{\partial x_\alpha \partial x_\gamma}=\frac{\partial \delta u_\beta}{\partial x_\alpha \delta\xi}\frac{\partial u_\delta}{\partial x_\gamma} \tag{A9}$$

Expanding the 9th term of Equation (A1)

$$\frac{\partial}{\partial x_\gamma}\left[\frac{\partial u_\beta}{\partial x_\alpha}\frac{\delta u_\delta}{\delta\xi}\right]-\frac{\partial^2 u_\beta}{\partial x_\gamma \partial x_\alpha}\frac{\delta u_\delta}{\delta\xi}=\frac{\partial u_\beta}{\partial x_\alpha}\frac{\partial \delta u_\delta}{\partial x_\gamma \delta\xi} \tag{A10}$$

Substituting Equation (A2) into the first term of Equation (A1) to demonstrate the integration by parts process used in this study.

$$\begin{aligned}
&\text{a)}\ \rho\int_{\tau_b}^{\tau_b}\frac{\mathrm{d}u_a}{\mathrm{d}t}\frac{\delta \mathrm{d}u_a}{\delta\xi \mathrm{d}t}\mathrm{d}t=\rho\int_{\tau_a}^{\tau_b}\frac{\mathrm{d}}{\mathrm{d}t}\left[\frac{\mathrm{d}u_a}{\mathrm{d}t}\frac{\delta u_a}{\delta\xi}\right]\mathrm{d}t-\rho\int_{\tau_a}^{\tau_b}\frac{\delta u_a}{\delta\xi}\frac{\mathrm{d}^2 u_a}{\mathrm{d}t^2}\mathrm{d}t\\
&\text{b)}\ \rho\int_{\tau_b}^{\tau_b}\frac{\mathrm{d}u_a}{\mathrm{d}t}\frac{\delta \mathrm{d}u_a}{\delta\xi \mathrm{d}t}\mathrm{d}t=\rho\left[\frac{\mathrm{d}u_a}{\mathrm{d}t}\frac{\delta u_a}{\delta\xi}\right]_{\tau_a}^{\tau_b}-\rho\int_{\tau_a}^{\tau_b}\frac{\delta u_a}{\delta\xi}\frac{\mathrm{d}^2 u_a}{\mathrm{d}t^2}\mathrm{d}t\\
&\text{c)}\ \rho\int_{\tau_b}^{\tau_b}\frac{\mathrm{d}u_a}{\mathrm{d}t}\frac{\delta \mathrm{d}u_a}{\delta\xi \mathrm{d}t}\mathrm{d}t=-\rho\int_{\tau_a}^{\tau_b}\frac{\delta u_a}{\delta\xi}\frac{\mathrm{d}^2 u_a}{\mathrm{d}t^2}\mathrm{d}t
\end{aligned} \tag{A11}$$

Because the variations $\frac{\delta u_\alpha}{\delta\xi}$ are equal to zero at the limit of integration, the first term on the right side of Equation (A11b) is equal to zero. Substituting the first terms of Equations (A2) to (A11) into Equation (A1).

$$\begin{aligned}
0=\frac{1}{2}\int_{s_a}^{s_b}\Bigg\{&\frac{\partial}{\partial x_\beta}\left[\frac{\delta u_\alpha}{\delta\xi}\frac{\partial u_\gamma}{\partial u_\delta}\right]+\frac{\partial}{\partial x_\delta}\left[\frac{\delta u_\gamma}{\delta\xi}\frac{\partial u_\alpha}{\partial u_\beta}\right]+\frac{\partial}{\partial x_\alpha}\left[\frac{\delta u_\beta}{\delta\xi}\frac{\partial u_\gamma}{\partial x_\delta}\right]\\
&+\frac{\partial}{\partial x_\delta}\left[\frac{\partial u_\alpha}{\partial x_\beta}\frac{\delta u_\gamma}{\delta\xi}\right]+\frac{\partial}{\partial x_\beta}\left[\frac{\partial u_\delta}{\partial x_\gamma}\frac{\delta u_\alpha}{\delta\xi}\right]+\frac{\partial}{\partial x_\gamma}\left[\frac{\partial u_\alpha}{\partial x_\beta}\frac{\delta u_\delta}{\delta\xi}\right]\\
&+\frac{\partial}{\partial x_\alpha}\left[\frac{\delta u_\beta}{\delta\xi}\frac{\partial u_\delta}{\partial x_\gamma}\right]+\frac{\partial}{\partial x_\gamma}\left[\frac{\partial u_\beta}{\partial x_\alpha}\frac{\delta u_\delta}{\delta\xi}\right]\Bigg\}\mathrm{d}v
\end{aligned} \tag{A12}$$

Because the variations in $\frac{\delta u_\alpha}{\delta\xi}$ are equal to zero at the limit of integration on the surfaces s_a and s_b, Equation (A12) is equal to zero. This is similar as was done in Equation (A11). Continuing with the substitution of the remaining terms of Equations (A2) to (A10) into Equation (A1).

$$\begin{aligned}
0=-\rho\int_{\tau_a}^{\tau_b}\frac{\delta u_\alpha}{\delta\xi}\frac{\mathrm{d}^2 u_\alpha}{\mathrm{d}t^2}\mathrm{d}t+\frac{1}{2}\int_{s_a}^{s_b}\Bigg[&c_{\alpha\beta\gamma\delta}\frac{\delta u_\alpha}{\delta\xi}\frac{\partial^2 u_\gamma}{\partial x_\beta \partial x_\delta}+c_{\gamma\beta\alpha\delta}\frac{\partial^2 u_\gamma}{\partial x_\delta \partial x_\beta}\frac{\delta u_\alpha}{\delta\xi}\\
&+c_{\beta\alpha\gamma\delta}\frac{\delta u_\alpha}{\delta\xi}\frac{\partial^2 u_\gamma}{\partial x_\beta \partial x_\delta}+c_{\gamma\beta\alpha\delta}\frac{\delta u_\alpha}{\delta\xi}\frac{\partial^2 u_\beta}{\partial x_\gamma \partial x_\delta}\\
&+c_{\alpha\beta\gamma\delta}\frac{\delta u_\alpha}{\delta\xi}\frac{\partial^2 u_\delta}{\partial x_\beta \partial x_\gamma}+c_{\delta\beta\gamma\alpha}\frac{\delta u_\alpha}{\delta\xi}\frac{\partial^2 u_\delta}{\partial x_\gamma \partial x_\beta}\\
&+c_{\beta\alpha\gamma\delta}\frac{\delta u_\alpha}{\delta\xi}\frac{\partial^2 u_\delta}{\partial x_\beta \partial x_\gamma}+c_{\delta\beta\gamma\alpha}\frac{\delta u_\alpha}{\delta\xi}\frac{\partial^2 u_\beta}{\partial x_\delta \partial x_\gamma}+2\rho g\delta_{2\alpha}\frac{\delta u_\alpha}{\delta\xi}\Bigg]\mathrm{d}v
\end{aligned} \tag{A13}$$

Since the all the quantities in Equation (A13) are scalars one can interchange subscripts.

$$\begin{aligned}0 = -\rho\int_{\tau_a}^{\tau_b}\frac{\delta u_\alpha}{\delta\xi}\frac{\mathrm{d}^2u_a}{\mathrm{d}t^2}\mathrm{d}t + \frac{1}{2}\int_{s_a}^{s_b}\Bigg[c_{\alpha\beta\gamma\delta}\frac{\partial^2u_\gamma}{\partial x_\beta\partial x_\delta}\frac{\delta u_\alpha}{\delta\xi} + c_{\gamma\beta\alpha\delta}\frac{\partial^2u_\gamma}{\partial x_\beta\partial x_\delta}\frac{\delta u_\alpha}{\delta\xi}\\ + c_{\beta\alpha\gamma\delta}\frac{\partial^2u_\gamma}{\partial x_\beta\partial x_\delta}\frac{\delta u_\alpha}{\delta\xi} + c_{\gamma\beta\alpha\delta}\frac{\partial^2u_\beta}{\partial x_\delta\partial x_\gamma}\frac{\delta u_\alpha}{\delta\xi}\\ + c_{\alpha\beta\gamma\delta}\frac{\partial^2u_\delta}{\partial x_\beta\partial x_\gamma}\frac{\delta u_\alpha}{\delta\xi} + c_{\delta\beta\gamma\alpha}\frac{\partial^2u_\delta}{\partial x_\beta\partial x_\gamma}\frac{\delta u_\alpha}{\delta\xi}\\ + c_{\beta\alpha\gamma\delta}\frac{\partial^2u_\delta}{\partial x_\beta\partial x_\gamma}\frac{\delta u_\alpha}{\delta\xi} + c_{\delta\beta\gamma\alpha}\frac{\partial^2u_\beta}{\partial x_\gamma\partial x_\delta}\frac{\delta u_\alpha}{\delta\xi} + \rho g\delta_{2\alpha}\frac{\delta u_\alpha}{\delta\xi}\Bigg]\mathrm{d}v\end{aligned} \tag{A14}$$

Factoring out $\frac{\delta u_\alpha}{\delta\xi}$

$$\begin{aligned}-\rho\int_{\tau_a}^{\tau_b}\frac{\delta u_\alpha}{\delta\xi}\frac{\mathrm{d}^2u_\alpha}{\mathrm{d}t^2}\mathrm{d}t + \frac{1}{2}\int_{s_a}^{s_b}\Bigg[c_{\alpha\beta\gamma\delta}\frac{\partial^2u_\gamma}{\partial x_\beta\partial x_\delta} + c_{\gamma\beta\alpha\delta}\frac{\partial^2u_\gamma}{\partial x_\delta\partial x_\beta}\\ + c_{\beta\alpha\gamma\delta}\frac{\partial^2u_\gamma}{\partial x_\delta\partial x_\beta} + c_{\gamma\beta\alpha\delta}\frac{\partial^2u_\beta}{\partial x_\delta\partial x_\gamma} + c_{\alpha\beta\gamma\delta}\frac{\partial^2u_\delta}{\partial x_\beta\partial x_\gamma} + c_{\delta\beta\gamma\alpha}\frac{\partial^2u_\delta}{\partial x_\gamma\partial x_\beta}\\ + c_{\beta\alpha\gamma\delta}\frac{\partial^2u_\delta}{\partial x_\beta\partial x_\gamma} + c_{\delta\beta\gamma\alpha}\frac{\partial^2u_\beta}{\partial x_\gamma\partial x_\delta} + \rho g\delta_{2\alpha}\Bigg]\frac{\xi u_\alpha}{\delta\xi}\mathrm{d}v = 0\end{aligned} \tag{A15}$$

Because the variation is arbitrary $\frac{\delta u_\alpha}{\delta\xi}$ the fundamental lemma of the Calculus of variation states that the terms in the square bracket multiplying the variation $\frac{\delta u_\alpha}{\delta\xi}$ must be equal to zero for Equation (A15) to be equal to zero.

$$\begin{aligned}\rho\frac{\mathrm{d}^2u_\alpha}{\mathrm{d}t^2} = \frac{1}{2}\Bigg[c_{\alpha\beta\gamma\delta}\frac{\partial^2u_\gamma}{\partial x_\beta\partial x_\delta} + c_{\gamma\beta\alpha\delta}\frac{\partial^2u_\gamma}{\partial x_\delta\partial x_\beta} + c_{\beta\alpha\gamma\delta}\frac{\partial^2u_\gamma}{\partial x_\delta\partial x_\beta}\\ + c_{\gamma\beta\alpha\delta}\frac{\partial^2u_\beta}{\partial x_\delta\partial x_\gamma} + c_{\alpha\beta\gamma\delta}\frac{\partial^2u_\delta}{\partial x_\beta\partial x_\gamma} + c_{\delta\beta\gamma\alpha}\frac{\partial^2u_\delta}{\partial x_\gamma\partial x_\beta}\\ + c_{\beta\alpha\gamma\delta}\frac{\partial^2u_\delta}{\partial x_\beta\partial x_\gamma} + c_{\delta\beta\gamma\alpha}\frac{\partial^2u_\beta}{\partial x_\gamma\partial x_\delta}\Bigg] + \frac{\partial\phi}{\partial u_\alpha}\end{aligned} \tag{A16}$$

Equation (A16) becomes Equation (8).

Appendix B

The gradients, divergence and curl in cylindrical coordinates are:

$$\text{a)}\ \nabla\phi = \hat{\boldsymbol{a}}_r \frac{\partial\phi}{\partial r} + \hat{\boldsymbol{a}}_\theta \frac{1}{r}\frac{\partial\phi}{\partial\theta} + \hat{\boldsymbol{a}}_z \frac{\partial\phi}{\partial z}$$

$$\text{b)}\ \nabla\bullet\boldsymbol{u} = \frac{1}{r}\frac{\partial}{\partial r}(ru_r) + \frac{1}{r}\frac{\partial u_\theta}{\partial\theta} + \frac{\partial u_z}{\partial z} \tag{B1}$$

$$\text{c)}\ \nabla\times\boldsymbol{u} = \hat{\boldsymbol{a}}_r\left(\frac{1}{r}\frac{\partial u_z}{\partial\theta} - \frac{\partial u_\theta}{\partial z}\right) + \hat{\boldsymbol{a}}_\theta\left(\frac{\partial u_r}{\partial z} - \frac{\partial u_z}{\partial r}\right) + \hat{\boldsymbol{a}}_z\left[\frac{1}{r}\frac{\partial}{\partial r}(ru_\theta) - \frac{1}{r}\frac{\partial u_r}{\partial\theta}\right]$$

The gradient of the divergent in cylindrical coordinates is:

$$\begin{aligned}\nabla(\nabla\bullet\boldsymbol{u}) = {}& \hat{\boldsymbol{a}}_r\left\{\frac{\partial}{\partial r}\left[\frac{1}{r}\frac{\partial}{\partial r}(ru_r)\right] + \frac{\partial}{\partial r}\left(\frac{1}{r}\frac{\partial u_\theta}{\partial\theta}\right) + \frac{\partial^2 u_z}{\partial r\partial z}\right\} \\ & + \hat{\boldsymbol{a}}_\theta\left[\frac{1}{r^2}\frac{\partial^2}{\partial\theta\partial r}(ru_r) + \frac{1}{r^2}\frac{\partial^2 u_\theta}{\partial\theta^2} + \frac{1}{r}\frac{\partial^2 u_z}{\partial\theta\partial z}\right] \\ & + \hat{\boldsymbol{a}}_z\left[\frac{1}{r}\frac{\partial^2}{\partial z\partial r}(ru_r) + \frac{1}{r}\frac{\partial^2 u_\theta}{\partial z\partial\theta} + \frac{\partial^2 u_z}{\partial z^2}\right]\end{aligned} \tag{B2}$$

The curl of the curl in cylindrical coordinates are:

$$\begin{aligned}\nabla\times\nabla\times\boldsymbol{u} = {}& \hat{\boldsymbol{a}}_r\left[\frac{1}{r^2}\frac{\partial}{\partial\theta\partial r}(ru_\theta) - \frac{1}{r^2}\frac{\partial^2 u_r}{\partial\theta^2} - \frac{\partial^2 u_r}{\partial z^2} + \frac{\partial^2 u_z}{\partial z\partial r}\right] \\ & + \hat{\boldsymbol{a}}_\theta\left\{\frac{1}{r}\frac{\partial^2 u_z}{\partial z\partial\theta} - \frac{\partial^2 u_\theta}{\partial z^2} - \frac{\partial}{\partial r}\left[\frac{1}{r}\frac{\partial}{\partial r}(ru_\theta)\right] + \frac{\partial}{\partial r}\left(\frac{1}{r}\frac{\partial u_r}{\partial\theta}\right)\right\} \\ & + \hat{\boldsymbol{a}}_z\left[\frac{1}{r}\frac{\partial}{\partial r}\left(r\frac{\partial u_r}{\partial z}\right) - \frac{1}{r}\frac{\partial}{\partial r}\left(r\frac{\partial u_z}{\partial r}\right) - \frac{1}{r^2}\frac{\partial^2 u_z}{\partial\theta^2} + \frac{1}{r}\frac{\partial^2 u_\theta}{\partial\theta\partial z}\right]\end{aligned} \tag{B3}$$

Calculating $\nabla^2\boldsymbol{u} = \nabla(\nabla\bullet\boldsymbol{u}) - \nabla\times\nabla\times\boldsymbol{u}$:

$$\begin{aligned}& \nabla(\nabla\bullet\boldsymbol{u}) - \nabla\times\nabla\times\boldsymbol{u} \\ & = \hat{\boldsymbol{a}}_r\left[\frac{1}{r}\frac{\partial u_r}{\partial r} + \frac{\partial^2 u_r}{\partial r^2} + \frac{1}{r^2}\frac{\partial^2 u_r}{\partial\theta^2} + \frac{\partial^2 u_r}{\partial z^2} - \frac{u_r}{r^2} - \frac{2}{r^2}\frac{\partial u_\theta}{\partial\theta}\right] \\ & + \hat{\boldsymbol{a}}_\theta\left[\frac{1}{r}\frac{\partial u_\theta}{\partial r} + \frac{\partial^2 u_\theta}{\partial r^2} + \frac{1}{r^2}\frac{\partial^2 u_\theta}{\partial\theta^2} + \frac{\partial^2 u_\theta}{\partial z^2} - \frac{u_\theta}{r^2} + \frac{2}{r^2}\frac{\partial u_r}{\partial\theta}\right] \\ & + \hat{\boldsymbol{a}}_z\left[\frac{1}{r}\frac{\partial u_z}{\partial r} + \frac{\partial^2 u_z}{\partial r^2} + \frac{1}{r^2}\frac{\partial^2 u_z}{\partial\theta^2} + \frac{\partial^2 u_z}{\partial z^2}\right]\end{aligned} \tag{B4}$$

Appendix C

The strain components in cylindrical coordinates are:

$$\text{a)}\ \Sigma_{rr} = \frac{\partial u_r}{\partial r} \qquad \text{b)}\ \Sigma_{\theta\theta} = \frac{u_r}{r} + \frac{1}{r}\frac{\partial u_\theta}{\partial\theta}$$

$$\text{c)}\ \Sigma_{zz} = \frac{\partial u_z}{\partial z} \qquad \text{d)}\ \Sigma_{r\theta} = \frac{1}{2}\left(\frac{\partial u_\theta}{\partial r} - \frac{u_\theta}{r} + \frac{1}{r}\frac{\partial u_r}{\partial\theta}\right) \tag{C1}$$

$$\text{e)}\ \Sigma_{rz} = \frac{1}{2}\left(\frac{\partial u_r}{\partial z} + \frac{\partial u_z}{\partial r}\right) \qquad \text{f)}\ \Sigma_{\theta z} = \frac{1}{2}\left(\frac{1}{r}\frac{\partial u_z}{\partial\theta} + \frac{\partial u_\theta}{\partial z}\right)$$

Appendix D

Recurrence relations for Modified Bessel Functions of the second kind

$$\frac{\mathrm{d}K_{\eta}(x)}{\mathrm{d}x} = -\frac{1}{2}\left[K_{\eta-1}(x) + K_{\eta+1}(x)\right] \tag{D1}$$

or

$$\frac{\mathrm{d}K_{\eta}(x)}{\mathrm{d}x} = -K_{\eta-1}(x) - \frac{\eta}{x}K_{\eta+1}(x) \tag{D2}$$

Asymptotic approximation of Modified Bessel Functions of the second kind.

$$\text{a)}\ K_{\eta}(x) \approx \sqrt{\frac{\pi}{2x}}\mathrm{e}^{-x}\left[1 + \frac{4\eta^2 - 1^2}{1(2x)}\left(1 + \frac{\left(4\eta^2 - 3\right)^2}{2(8x)}\left(1 + \frac{4\eta^2 - 5^2}{3(8x)}(1 + \cdots)\right)\right)\right]$$

$$\text{b)}\ K_{0}(x) \approx \sqrt{\frac{\pi}{2x}}\mathrm{e}^{-x}\left[1 - \frac{1}{8x}\left(1 - \frac{9}{2(8x)}\left(1 - \frac{25}{3(8x)}\right)\right)\right] \tag{D3}$$

$$\text{c)}\ K_{1}(x) \approx \sqrt{\frac{\pi}{2x}}\mathrm{e}^{-x}\left[1 + \frac{3}{8x}\left(1 - \frac{5}{2(8x)}\left(1 - \frac{21}{3(8x)}\right)\right)\right]$$